International Journal of Computational Intelligence and Applications
Vol. 18, No. 2 (2019) 1950012 (20 pages)

DOI: 10.1142/S1469026819500123

Backstepping Sliding Mode Controller Improved with Interval Type-2 Fuzzy Logic Applied to the Dual Star Induction Motor

Hilal Rahali[*,§], Samir Zeghlache[†,¶], Loutfi Benyettou[*,‖] and Leila Benalia[‡,**]

[*]*Laboratoire de Genie Élecrtique*
Department of Electrical Engineering
Faculty of Technology
University Mohamed Boudiaf of M'sila
BP 166, Ichbilia 28000, Algeria

[†]*Laboratoire d'analyse des Signaux et Systèmes*
Department of Electrical Engineering
Faculty of Technology
University Mohamed Boudiaf of M'sila
BP 166, Ichbilia 28000, Algeria

[‡]*Laboratoire de Genie Elecrtique*
Department of Electrical Engineering
Batna-2 University
Street Chahid Med, El Hadi Boukhlouf, Algeria
[§]*hilal_lami@yahoo.fr; hilal.rahali@univ-msila.dz*
[¶]*samir.zeghlache@univ-msila.dz*
[‖]*loutfi.benyettou@univ-msila.dz*
[**]*leila_bena@yahoo.fr*

Received 8 February 2019
Revised 2 April 2019
Accepted 29 April 2019
Published 28 June 2019

This paper proposes Interval type-2 Fuzzy sliding mode controller based on Backstepping (IT2FBSMC), to control the speed of a dual star induction machine (DSIM), in order to get a robust performance machine. An appropriate control strategy based on the coupling of three methods (Backstepping, sliding mode and type-2 Fuzzy controller) is used to build a robust controller used to approximate the discontinuous control eliminating the chattering phenomenon and guaranteeing the stability of the machine. Moreover, it forces the rotor angular speed to follow a desired reference signal. The simulation results obtained using Matlab/Simulink behavior are presented and discussed. The obtained results show that the controller can greatly alleviate the chattering effect and enhance the robustness of control systems with high accuracy.

Keywords: Interval type-2 fuzzy; sliding mode; backstepping; chattering phenomenon; speed control.

[§]Corresponding author.

1. Introduction

In industrial applications, dual star induction machine (DSIM) has been used instead of traditional three-phase induction machine for improving its reliability due to its performances in high power fields and high power applications.[1–3] In the last years, the DSIM speed control has been the subject of investigations, and its characteristics, performances, modeling and control are explained in detail in Refs. 1, 2 and 4–7.

The dual stator induction machine requires a dual three-phase power supply coupled by two voltage source inverters (VSIs) being very reliable for robust variable speed operation[1,6] and which has many advantages such as reduced torque pulsation and reduced rotor harmonics as they can be filtered. The most important advantage is the usage of less powerful electronic components which allow a higher commutation frequency as the current flowing in a six-phase machine is less than that flowing in a three-phase machine.[1–4,8] It is used as motor or generator particularly in autonomous system, such as electric hybrid vehicles, locomotive traction, electric ship propulsion, etc.[1,7–9] Moreover, DSIM does not need any maintenance because it is magnetless and brushless, so it is an economical machine.[1]

Among the most widely used methods is the sliding mode control (SMC) method, which has been applied to robust control of uncertain nonlinear systems.[10,11] It is widely used to obtain good dynamic performance of controlled systems especially in complicated environment and systems with uncertainty disturbance[12]; this approach presents robustness to parameter variations and insensitivity to external disturbances as well as the ability to globally stabilize the system in the presence of other disturbances.[13]

Recently, the SMC of nonlinear systems remains an important area of research in the field of machine control. However, its major drawback is the chattering phenomenon. Considerable efforts and different works are carried out for motor system based on SMC, namely a new PI fuzzy sliding mode controller of DSIM,[14] fuzzy sliding mode speed controller of induction motor,[15] SMC of a dual stator induction generator.[16]

Backstepping control (BSC) is a newly developed non linear control strategy, based on Lyapunov theory, the current form of BSC is developed by Freeman *et al.*[17,18]

Many newer researches address the idea of the hybrid control based on appropriate combination of fuzzy logic approach with various nonlinear control methodologies.[14,15] These control techniques without the use of intelligent methods such as fuzzy logic cannot guarantee good robustness, stability and performance in all different systems. Several methods have been made, including type-1 fuzzy logic. In Refs. 14 and 19, the authors presented a hybrid control based on type-1 fuzzy

sliding mode controller for DSIM and the proposed control in this paper can be attenuated by the chattering phenomenon of the SMC. In, Ref. 1, the type-1 fuzzy logic controller is proposed to stabilize the DSIM, using the control strategy fuzzy logic, and to adjust the drive system speed. In, Ref. 20, the authors presented the hybrid control composed by neuro-fuzzy (NF)-based auto-tuning proportional integral controller for indirect field-controlled induction motor drive, while the NF parameters have been updated online through the use of training algorithm. The high performances of this control strategy and their robustness have been confirmed in simulation results.

The combination of three recent methods based on backstepping, SMC (BSMC) and interval type-2 fuzzy control (IT2FLC) represents a contribution of this work. The IT2FLC is used to approximate the discontinuous control and reduce the chattering phenomenon, and the method adopted here will guarantee the system trajectories moving toward and staying on the sliding surface $S_i = 0$. So, an effective and robust controller is developed for DSIM subjected to external disturbances. The proposed IT2FBSMC strategy will improve the performance of DSIM with external disturbances and guarantees the stability of this machine using Lyapunov theorem.

The objective of the proposed IT2FBSMC strategy is to control rotor magnitude flux and to force the rotor angular speed to follow a desired reference signal.

The remainder of the paper is organized as follows. The system description and modeling of the DSIM is given in Sec. 2. The background of type-2 fuzzy control logic is proposed in Sec. 3. Section 4 explains the principles of IT2FSMC based on backstepping for regulating the speed of the DSIM. Simulation results what used the proposed IT2FBSMC are presented in Section 5. Finally, conclusion is given in Sec. 6.

2. Description and Modeling of DSIM

The windings of the dual star induction machine are represented in Fig. 1, the DSIM is composed by two stars separate with three phases winding fixed and standard simple squirrel-cage rotor composed three rotors phases moving. The two stators are displaced by angle ($\alpha = \pi/6$), their axes are shifted from each other by an electrical angle equal to ($2\pi/3$) with isolated neutrals.[1,2,6,16,21] Therefore, the orthogonality created between the two oriented fluxes, which must be strictly observed, leads to the generation of the decoupled control with an optimal torque.[21,22]

Table 1 shows the nomenclature of the parameters in DSIM model.

2.1. *DSIM model*

The Park model of DSIM in a (d–q) rotating frame is presented as follows.

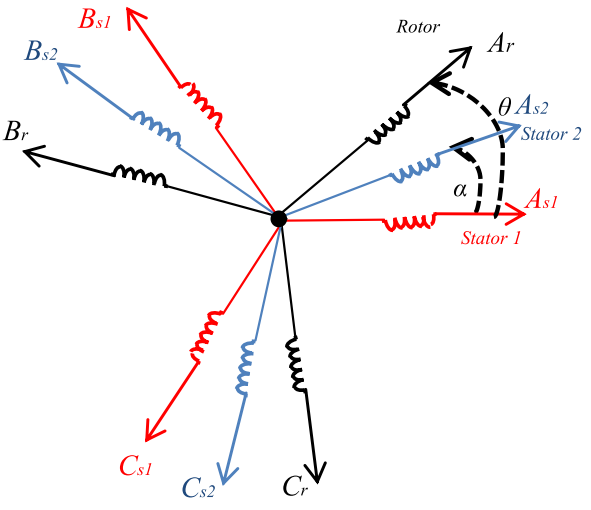

Fig. 1. Representation of the DSIM winding.

Electrical equations of the DSIM are given by

$$\begin{cases} V_{ds1} = R_{s1} i_{ds1} + \dfrac{d}{dt}\varphi_{ds1} - \omega_s \varphi_{qs1}, \\ V_{qs1} = R_{s1} i_{qs1} + \dfrac{d}{dt}\varphi_{qs1} + \omega_s \varphi_{ds1}, \\ V_{ds2} = R_{s2} i_{ds2} + \dfrac{d}{dt}\varphi_{ds2} - \omega_s \varphi_{qs2}, \\ V_{qs2} = R_{s2} i_{qs2} + \dfrac{d}{dt}\varphi_{qs2} + \omega_s \varphi_{ds2}, \\ 0 = R_r i_{dr} + \dfrac{d}{dt}\varphi_{dr} + (\omega_s - \omega_r)\varphi_{qr}, \\ 0 = R_r i_{qr} + \dfrac{d}{dt}\varphi_{qr} + (\omega_s - \omega_r)\varphi_{dr}. \end{cases} \tag{1}$$

Table 1. Nomenclature of the parameters in DSIM model.

V_{ds}, V_{qs}, V_{dr}, V_{qr}	stator and rotor voltages d–q-axis components
i_{ds}, i_{qs}, i_{dr}, i_{qr}	stator and rotor currents d–q-axis components
φ_s, φ_r	stator–rotor flux
φ_d, φ_q	stator flux d–q-axis components
ω_s, ω_r	stator and rotor pulsation, respectively
ω_{sref}, ω_{rref}	stator and rotor pulsation references, respectively
φ_{rref}	rotor flux control reference
R_s, R_r	stator–rotor resistance

Table 1. (*Continued*)

T_r	load torque
ω	mechanical speed
ω_{glref}	sliding speed reference
C_{em}	electromagnetic torque
L_s, L_r	stator and rotor inductance, respectively
L_m	mutual inductance
J	total inertia
p	number of pole pairs
K_f	friction coefficient

Expression of the electromagnétique torque of DSIM is given by

$$C_{em} = p\frac{L_m}{L_m + L_r}[\varphi_{dr}(i_{qs1} + i_{qs2}) - \varphi_{qr}(i_{ds1} + i_{ds2})]. \tag{2}$$

In field-oriented control (FOC), the flux vector is forced to align with the d-axis ($\phi_q = 0$) in order to have decoupling model which is similar to a DC motor. The DSIM state equations in the reference (d, q) are given by

$$\begin{cases} \dot{i}_{ds1} = \dfrac{1}{L_{s1}}(V_{ds1} - R_{s1}i_{ds1} + \omega_s(L_{s1}i_{qs1} + T_r\phi_{\text{rref}}\omega_{\text{glref}})), \\ \dot{i}_{qs1} = \dfrac{1}{L_{s1}}(V_{qs1} - R_{s1}i_{qs1} - \omega_s(L_{s1}i_{ds1} + \phi_{\text{rref}})), \\ \dot{i}_{ds2} = \dfrac{1}{L_{s2}}(V_{ds2} - R_{s2}i_{ds2} + \omega_s(L_{s2}i_{qs2} + T_r\phi_{\text{rref}}\omega_{\text{glref}})), \\ \dot{i}_{qs2} = \dfrac{1}{L_{s2}}(V_{qs2} - R_{s2}i_{qs2} - \omega_s(L_{s2}i_{ds2} + \phi_{\text{rref}})), \\ \dot{\Omega} = \dfrac{1}{j}\left(p\dfrac{L_m}{L_m + L_r}\phi_{\text{rref}}(i_{qs1} + i_{qs2}) - C_r - K_f\Omega\right), \\ \dot{\phi}_r = \dfrac{-R_r}{L_m + L_r}\phi_r + \dfrac{L_m \cdot R_r}{L_m + L_r}(i_{ds1} - i_{ds2}). \end{cases} \tag{3}$$

The FOC-based conventional PI speed controller is required in some industrial processes. It is easy to design and implement. However present difficulty is in terms of dealing with parameter variations and load disturbances.[21,23] Later, if leads to a big loss of control performance. To overcome these problems, a robust control strategy based on synthesis of the hybrid (backstepping, sliding mode and interval type-2 fuzzy) control with a sliding surface to dual star induction motor for speed and flux control is proposed.

3. Background of Type-2 Fuzzy Logic Control

Type-1 and type-2 fuzzy logics are mainly similar.[24] However, there exist two essential differences between them which are the membership function shape and the

output processor. Interval type-2 fuzzy controller is very effective in cases where it is difficult to determine an exact membership function for a fuzzy set.[24]

3.1. *Fuzzifier*

The fuzzifier maps the crisp input vector $(e_1, e_2, e_n)^T$ to a type-2 fuzzy system $\tilde{\mathrm{A}}_x$, very similar to the procedure performed in a type-1 fuzzy logic system.

3.2. *Rules*

The general form of the ith rule of the type-2 fuzzy logic system can be written as

$$\begin{aligned} &\text{If } e_1 \text{ is } \tilde{F}_1^i \quad \text{and} \quad e_2 \text{ is } \tilde{F}_1^i \quad \text{and} \quad \ldots e_n \text{ is } \tilde{F}_n^i, \\ &\text{then } y^i = \tilde{G}^i, \quad i = 1, \ldots, M, \end{aligned} \tag{4}$$

where $\tilde{F}_{ij}$ represents the type-2 fuzzy system of the input state j of the ith rule, $x_1, x_2, \ldots, x_n$ are the inputs, $\tilde{G}^i$ is the output of type-2 fuzzy system for the rule i, and M is the number of rules. As can be seen, the rule structure of type-2 fuzzy logic system is similar to type-1 fuzzy logic system except that type-1 membership functions are replaced with their type-2 counterparts.

3.3. *Inference engine*

In fuzzy system interval type-2 using the minimum or product t-norms operations, the ith activated rule $F^i(x_1, \ldots, x_n)$ gives us the interval that is determined by two extremes $\underline{f}^i(x_1, \ldots, x_n)$ and $\overline{f}^i(x_1, \ldots, x_n)$ (see Ref. 25):

$$F^i(x_1, \ldots x_n) = [\underline{f}^i(x_1, \ldots x_n), \overline{f}^i(x_1, \ldots x_n)] \equiv [\underline{f}^i, \overline{f}^i] \equiv [\underline{f}^i, \overline{f}^i] \tag{5}$$

with: $\underline{f}^i$ and $\overline{f}^i$ are given as

$$\begin{aligned} \underline{f}^i &= \underline{\mu}_{F_1^i}(x_1) * \cdots * \underline{\mu}_{F_n^i}(x_n), \\ \overline{f}^i &= \bar{\mu}_{F_1^i}(x_1) * \cdots * \bar{\mu}_{F_n^i}(x_n). \end{aligned} \tag{6}$$

3.4. *Type reducer*

The obtained type-2 fuzzy system resulting in type-1 fuzzy system is computed. In this part, the available methods to compute the centroid of type-2 fuzzy system using the extension principle[26] are discussed. The centroid of type-1 fuzzy system A is given by

$$C_A = \frac{\sum_{i=1}^n z_i w_i}{\sum_{i=1}^n w_i}, \tag{7}$$

where n represents the number of discretized domain of A, $z_i \epsilon R$ and $w_i \epsilon [0, 1]$.

If each z_i and w_i are replaced with a type-1 fuzzy system Z_i and W_i, with associated membership functions of $\mu_z(z_i)$ and $\mu_w(W_i)$, respectively, by using the

extension principle, the generalized centroid for type-2 fuzzy system $\tilde{A}$ is given by

$$GC_{\tilde{A}} = \int_{z_1 \in Z_1} \cdots \int_{z_n \in Z_n} \int_{w_1 \in W_1} \cdots \int_{w_n \in W_n} [T_{i=1}^{n} \mu_Z(z_i) * T_{i=1}^{n} \mu_W(z_i)] \Big/ \frac{\sum_{i=1}^{n} z_i w_i}{\sum_{i=1}^{n} w_i}, \tag{8}$$

where $\mu_Z(z_i)$ and $\mu_W(W_i)$ are the associated membership functions. T is a t-norm and $GC_{\tilde{A}}$ is a type-1 fuzzy system.

For an interval type-2 fuzzy system,

$$\begin{aligned} GC_{\tilde{A}} &= [y_l(x), y_r(x)] \\ &= \int_{y^1 \in [y_l^1, y_r^1]} \cdots \int_{y^M \in [y_l^M, y_r^M]} \cdots \int_{f^1 \in [\underline{f}^1, \overline{f}^1]} \cdots \int_{f^M \in [\underline{f}^M, \overline{f}^M]} 1 \Big/ \frac{\sum_{i=1}^{M} f^i y^i}{\sum_{i=1}^{M} f^i}. \end{aligned} \tag{9}$$

3.5. *Deffuzzifier*

To get a crisp output from a type-1 fuzzy logic system, the type-reduced set must be defuzzied.

We have used the center of area defuzzification for the calculation of the value of output u_f:

$$u_f = \frac{\sum_{i=1}^{5} C_{fi} \mu_i(s)}{\sum_{i=1}^{5} \mu_i(s)}, \tag{10}$$

where C_{fi} is the center of the membership functions of u_f.

4. Interval Type-2 Fuzzy SMC Based on Backstepping (IT2FBSMC) Design

The SCM is an effective control strategy in modern control because of its robustness and simple realization; it consists in bringing the state trajectory of a system toward a chosen manifold in the state space called the sliding surface and making it switch by means of a suitable switching logic around it to the equilibrium point.[27]

A problem of the conventional sliding mode controller technique produces high frequency oscillations and dangerous vibrations in its outputs called chattering. Chattering is undesirable in conventional sliding mode controller in practice because it can excite the high frequency dynamics of the system.[19,28] In order to guarantee the performance, stability and robustness of the sliding mode controller to the uncertainties, we need to eliminate the chattering effect.

The basic idea of the backstepping control (BSC) design is that it can effectively linearize a nonlinear system such as DSIM in the presence of uncertainties. The BSC decomposes the global law of control by dividing the backstepping design into various design steps using the intermediate control (virtual control) result in each step dealing with a single-input–single-output design problem, and each step as reference

signal for the next design step until the completion of the control design (actual control). The objective of the controller is to build an adequate function of Lyapunov guaranteeing that the system is asymptotically stable and to achieve the objective tracking.

The recursive nature of the proposed control design is similar to the standard backstepping methodology. However, the proposed control design uses backstepping to design virtual controllers with a zero-order sliding surface at each recursive step. The benefit of this approach is that each virtual controller can compensate for unknown bounded function which contains unmodeled dynamics and external disturbances.[28]

The proposed idea of interval type-2 fuzzy SMC based on backstepping (IT2FBSMC) contains an equivalent control part and single-input–single-output interval type-2 fuzzy logic is used to approximate the discontinuous control and to improve the overshoot and settling time. The block diagram of the IT2FBSMC is shown in Fig. 2; it contains an equivalent control part and single-input–single-output interval type-2 fuzzy logic.

The SMC law can be represented as $u = u_{\text{eq}} + u_s$; the equivalent control u_{eq} is expressed, considering that the derivative of the surface is zero $\dot{S} = 0$ and the discontinuous control u_s is computed by

$$u_s = K_{fs} u_{fs}, \tag{11}$$

$$u_{fs} = \text{IT2FLC}, \tag{12}$$

where u_{fs} is the output of the IT2FLC, which is obtained by the normalized s, and K_{fs} is the normalization factor of the output variable.

Figure 3 illustrates such a concept, in which five labels of fuzzy sets are assigned to the input sliding variable s (NB; NM; ZE; PM; PB) which mean negative big, negative medium, zero, positive medium and positive big, respectively. All the membership functions of the fuzzy input linguistic variable Si is chosen to be triangular and trapezoidal.

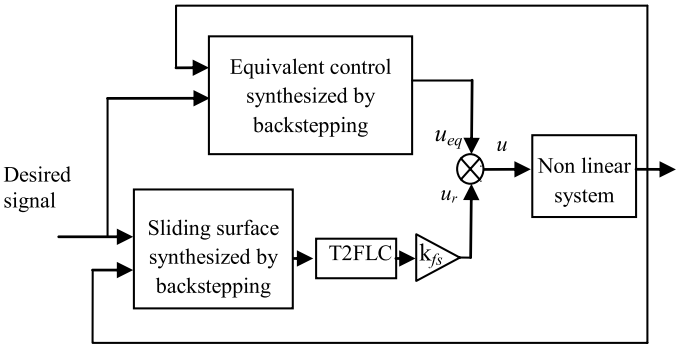

Fig. 2. Block diagram of the IT2FBSMC.

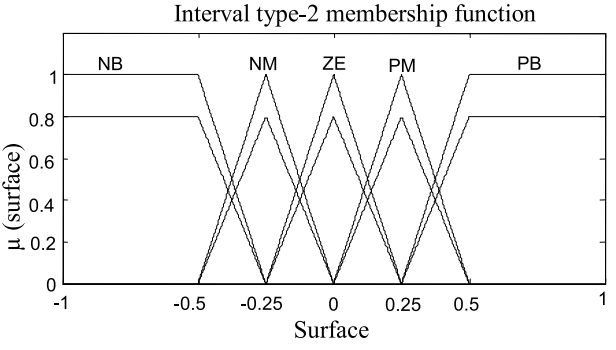

(a)

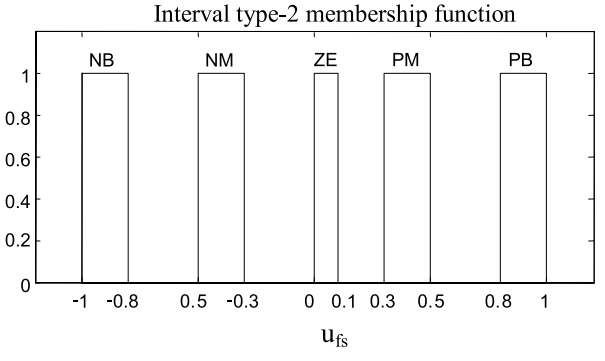

(b)

Fig. 3. Membership functions of input s and output u_{fs}.[28]

For the output discontinuous control u_{fs}, the labels of the fuzzy sets are also five (NB; NM; ZE; PM; PB) which mean negative big, negative medium, zero, positive medium and positive big, respectively. The fuzzy type-2 membership functions of the input and output are presented in Fig. 3.

Table 2 presents the rule's base which contains five rules.

The membership functions for the inputs and the outputs are defined in the range $[-1, 1]$, therefore, $|u_{fs}| \leq 1$.

u_{fs} given in (4) satisfies the following condition:

$$su_{fs} = -K^+|s|, \tag{13}$$

where $K^+ > 0$ is positive constant determined by a fuzzy type-2 inference system.

Table 2. Fuzzy rules for type-2 FLCs.[28]

	Rule 1	Rule 2	Rule 3	Rule 4	Rule 5
Surface	PB	PM	ZE	NM	NB
u_{fs}	NB	NM	ZE	PM	PB

Proof. The discontinuous control laws are computed by type-2 fuzzy logic inference using (20) and the iterative Karnik Mendel algorithms are presented in Refs. 29 and 30, where $\alpha_i = [\alpha_{\text{ilow}}, \alpha_{\text{iup}}]$ for $i = [1, \ldots, 5]$ is the membership interval of rules 1 to 5 presented in Table 2. Moreover, u_{fs} can be further analyzed as the following six conditions given thereafter. Only one of the six conditions will occur for any value of the sliding surface s.[28] □

Condition 1
Only rule 1 is activated ($s > 0.5, \alpha_1 = [0.8, 1], \alpha_j = [0, 0]$ for $j = 2, 3, 4, 5$)

$$u_{fs} = \text{T2FLC}(s) = \frac{-0.8 - 1}{2} = -0.9. \tag{14}$$

Condition 2
Rules 1 and 2 are activated: ($0.25 < s < 0.5, \alpha_1 = [\alpha_{1\text{low}}, \alpha_{1\text{up}}], \alpha_2 = [\alpha_{2\text{low}}, \alpha_{2\text{up}}], \alpha_j = [0, 0]$ for $j = 3, 4, 5$)
$0 \leq \alpha_{1\text{low}}, \alpha_{2\text{low}} \leq 0.8$ and $0 \leq \alpha_{1\text{up}}, \alpha_{2\text{up}} \leq 1$

$$u_{fs} = \text{T2FLC}(s) = \frac{1}{2}\left(\frac{-0.8\alpha_{1\text{low}} - 0.3\alpha_{2\text{up}}}{\alpha_{1\text{low}} + \alpha_{2\text{up}}} + \frac{-\alpha_{1\text{up}} - 0.5\alpha_{2\text{low}}}{\alpha_{1\text{up}} + \alpha_{2\text{low}}}\right). \tag{15}$$

Condition 3
Rules 2 and 3 are activated: $0 < s < 0.25, \alpha_2 = [\alpha_{2\text{low}}, \alpha_{2\text{up}}], \alpha_3 = [\alpha_{3\text{low}}, \alpha_{3\text{up}}], \alpha_j = [0, 0]$ for $j = 1, 4, 5$)
$0 \leq \alpha_{2\text{low}}, \alpha_{3\text{low}} \leq 0.8$ and $0 \leq \alpha_{2\text{up}}, \alpha_{3\text{up}} \leq 1$

$$u_{fs} = \text{T2FLC}(s) = \frac{1}{2}\left(\frac{-0.3\alpha_{2\text{low}} + 0.1\alpha_{3\text{up}}}{\alpha_{2\text{low}} + \alpha_{3\text{up}}} + \frac{-0.5\alpha_{2\text{up}}}{\alpha_{2\text{up}} + \alpha_{3\text{low}}}\right). \tag{16}$$

Condition 4
Rules 3 and 4 are activated: ($-0.25 < s < 0, \alpha_3 = [\alpha_{3\text{low}}, \alpha_{3\text{up}}], \alpha_4 = [\alpha_{4\text{low}}, \alpha_{4\text{up}}], \alpha_j = [0, 0]$ for $j = 1, 2, 5$)
$0 \leq \alpha_{3\text{low}}, \alpha_{4\text{low}} \leq 0.8$ and $0 \leq \alpha_{4\text{up}}, \alpha_{4\text{up}} \leq 1$

$$u_{fs} = \text{T2FLC}(s) = \frac{1}{2}\left(\frac{0.1\alpha_{3\text{low}} + 0.5\alpha_{4\text{up}}}{\alpha_{3\text{low}} + \alpha_{4\text{up}}} + \frac{0.3\alpha_{4\text{low}}}{\alpha_{3\text{up}} + \alpha_{4\text{low}}}\right). \tag{17}$$

Condition 5
Rules 4 and 5 are activated: ($-0.5 < s < -0.25, \alpha_4 = [\alpha_{4\text{low}}, \alpha_{4\text{up}}]$, $\alpha_5 = [\alpha_{5\text{low}}, \alpha_{5\text{up}}]$, $\alpha_j = [0, 0]$ for $j = 1, 2, 3$)
$0 \leq \alpha_{4\text{low}}, \alpha_{4\text{low}} \leq 0.8$ and $0 \leq \alpha_{5\text{up}}, \alpha_{5\text{up}} \leq 1$

$$u_{fs} = \text{T2FLC}(s) = \frac{1}{2}\left(\frac{0.5\alpha_{4\text{low}} + \alpha_{5\text{up}}}{\alpha_{4\text{low}} + \alpha_{5\text{up}}} + \frac{0.3\alpha_{4\text{up}} + 0.8\alpha_{5\text{low}}}{\alpha_{4\text{up}} + \alpha_{5\text{low}}}\right). \tag{18}$$

Condition 6

Only rule 5 is activated ($s < -0.5, \alpha_5 = [0.8, 1], \alpha_j = [0, 0]$ for $j = 1, 2, 3, 4$)

$$u_{fs} = \text{IT2FLC}(s) = \frac{1 + 0.8}{2} = 0.9. \tag{19}$$

According to six possible conditions shown in (33)–(38) we conclude

$$su_{fs} = s\text{T2FLC}(s) = -K^+|s| \tag{20}$$

With

$$K^+ = \begin{cases} 0.9 \quad \text{if} \quad s > 0.5 \quad \text{and} \quad s < -0.5, \\ \left|\frac{1}{2}\left(\frac{-0.8\alpha_{1\text{low}} - 0.3\alpha_{2\text{up}}}{\alpha_{1\text{low}} + \alpha_{2\text{up}}} + \frac{-\alpha_{1\text{up}} - 0.5\alpha_{2\text{low}}}{\alpha_{1\text{up}} + \alpha_{2\text{low}}}\right)\right| & \text{if} \quad 0.25 < s < 0.5, \\ \left|\frac{1}{2}\left(\frac{-0.3\alpha_{2\text{low}} + 0.1\alpha_{3\text{up}}}{\alpha_{2\text{low}} + \alpha_{3\text{up}}} + \frac{-0.5\alpha_{2\text{up}}}{\alpha_{2\text{up}} + \alpha_{3\text{low}}}\right)\right| & \text{if} \quad 0 < s < 0.25, \\ \left|\frac{1}{2}\left(\frac{0.1\alpha_{3\text{low}} + 0.5\alpha_{4\text{up}}}{\alpha_{3\text{low}} + \alpha_{4\text{up}}} + \frac{0.3\alpha_{4\text{low}}}{\alpha_{3\text{up}} + \alpha_{4\text{low}}}\right)\right| & \text{if} \quad -0.25 < s < 0, \\ \left|\frac{1}{2}\left(\frac{0.5\alpha_{4\text{low}} + \alpha_{5\text{up}}}{\alpha_{4\text{low}} + \alpha_{5\text{up}}} + \frac{0.3\alpha_{4\text{up}} + 0.8\alpha_{5\text{low}}}{\alpha_{4\text{up}} + \alpha_{5\text{low}}}\right)\right| & \text{if} -0.5 < s < -0.25. \end{cases} \tag{21}$$

In Fig. 2, the control law is computed by

$$u = u_{\text{eq}} + u_s = u_{\text{eq}} + k_{fs}u_{fs}. \tag{22}$$

Then, sliding condition can be rewritten as follows:

$$s\dot{s} = -k_{fs}K^+|s| < 0 \tag{23}$$

or

$$\dot{s} = -k_{fs}\text{T2FLC}(s). \tag{24}$$

We show that the dynamic equations of the DSIM are nonlinear, therefore, give a complex control which is difficult to conceive. To avoid this complexity, a backstepping controller mechanism for the rotor speed regulation and the rotor flux generation can be applied.

The objective of the reverse controller is to build an adequate Lyapunov function guaranteed that the system is asymptotically stable and achieves the objective tracking. The final Lyapunov function associate is the sum of all Lyapunov functions adapted at each backstepping stage.[31,32] So, the overall stability and performance are achieved by Lyapunov theory for the whole system.

The block diagram of the proposed IT2FBSMC is shown in Fig. 4.

The synthesis of the hybrid (backstepping, sliding mode and IT2FLC) control with a sliding surface to dual star induction motor can be achieved in two successive steps.[32–34]

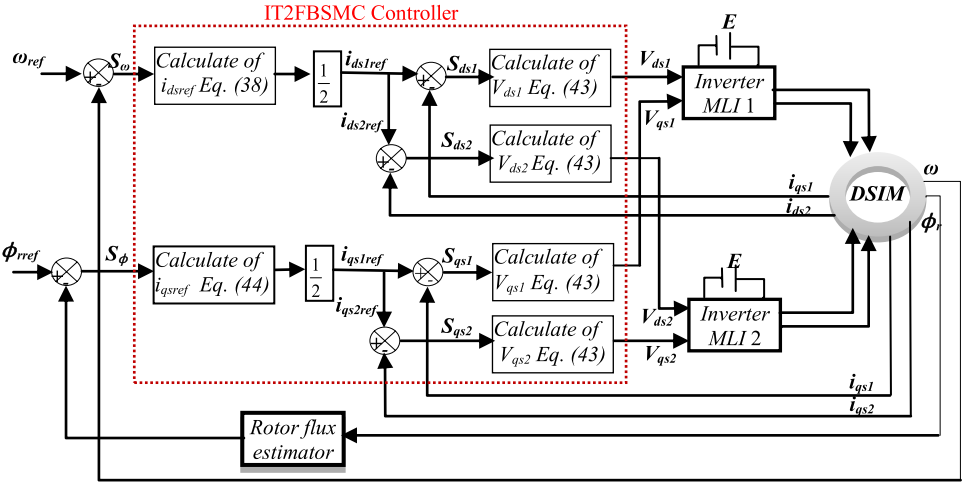

Fig. 4. Block diagram of the proposed T2FBSMC.

Step 1: *Speed and Flux regulators*

The equivalent control of the speed and the rotor flux module is computed as follow:

$$\dot{s} = \begin{cases} S_w = 0, \\ S_\varphi = 0. \end{cases} \tag{25}$$

The rotor speed and the rotor flux surface S_ω and S_ϕ are defined by

$$\begin{cases} S_w = \omega_{\text{ref}} - \omega_r, \\ S_\varphi = \phi_{\text{ref}} - \phi_r. \end{cases} \tag{26}$$

Derivative of the sliding surface S_ω and S_φ are calculated by

$$\begin{cases} \dot{S}_\omega = \dot{\omega}_{\text{rref}} - \dot{\omega}_r, \\ \dot{S}_\phi = \dot{\phi}_{rref} - \dot{\phi}_r. \end{cases} \tag{27}$$

Replacing the derivate of the speed ω_r and flux ϕ from (3) in (27), thus, one obtains the following equations:

$$\dot{S}_\omega = \dot{\omega}_{\text{rref}} - \frac{p^2}{j}\frac{L_m}{L_m + L_r}\phi_{\text{rref}}(i_{qs1} + i_{qs2}) + C_r\frac{p}{j} + \frac{K_f}{j}\omega_r, \tag{28}$$

$$\dot{S}_\phi = \dot{\phi}_{\text{rref}} + \frac{R_r}{L_m + L_r}\phi_r - \frac{R_r L_m}{L_m + L_r}(i_{ds1} + i_{ds2}). \tag{29}$$

We define the first function of Lyapunov V_1 which constitutes the speed and flux sliding surface as follows:

$$V_1 = \frac{1}{2}(S_\omega^2 + S_\phi^2). \tag{30}$$

The time derivative of (29) is obtained by

$$\dot{V}_1 = S_\omega \dot{S}_\omega + S_\phi \dot{S}_\phi. \tag{31}$$

Accounting to (28) and (29), one can rewrite (31) as follows:

$$\begin{aligned}\dot{V}_1 = S_\omega &\left\{\dot{\omega}_{\text{rref}} - \frac{p^2}{j}\frac{L_m}{L_m + L_r}\phi_{\text{rref}}(i_{qs1} + i_{qs2}) + C_r\frac{p}{j} + \frac{K_f}{j}\omega_r\right\} \\ &+ S_\phi\left\{\dot{\phi}_{\text{rref}} + \frac{R_r}{L_m + L_r}\phi_r - \frac{R_r L_m}{L_m + L_r}(i_{ds1} + i_{ds2})\right\}.\end{aligned} \tag{32}$$

According to the required slip condition obtained in (24), we propose,

$$\dot{\omega}_{\text{rref}} - \frac{p^2}{j}\frac{L_m}{L_m + L_r}\phi_{\text{rref}}(i_{qs1} + i_{qs2}) + C_r\frac{p}{j} + \frac{K_f}{j}\omega_r = -K_{fs\omega}\text{T2FLC}(S_\omega), \tag{33}$$

$$\dot{\phi}_{\text{rref}} + \frac{R_r}{L_m + L_r}\phi_r - \frac{R_r L_m}{L_m + L_r}(i_{ds1} + i_{ds2}) = -K_{fs\phi}\text{T2FLC}(S_\phi). \tag{34}$$

Assuming that $i_{ds1\text{ref}} + i_{ds2\text{ref}} = 2i_{ds1\text{ref}} = i_{ds\text{ref}}$ So $i_{ds1\text{ref}} = i_{ds2\text{ref}} = \frac{1}{2}i_{ds\text{ref}}$.

So, (34) becomes

$$\dot{\phi}_{\text{rref}} + \frac{R_r}{L_m + L_r}\phi_r + K_{fs\phi}\text{T2FLC}(S_\phi) = \frac{R_r L_m}{L_m + L_r}i_{ds\text{ref}}. \tag{35}$$

Finally, the reference current i_{ds} is determinated from the following expression:

$$i_{ds\text{ref}} = \left(\dot{\phi}_{\text{rref}} + \frac{R_r}{L_m + L_r}\phi_r + K_{fs\phi}\text{T2FLC}(S_\phi)\right)\frac{L_m + L_r}{R_r L_m}. \tag{36}$$

Similar to the $I_{ds\text{ref1}}$ case, (33) becomes

$$\dot{\omega}_{\text{rref}} + C_r\frac{p}{j} + \frac{K_f}{j}\omega_r + K_{fs\omega}\text{T2FLC}(S_\omega) = \frac{p^2}{j}\frac{L_m}{L_m + L_r}\phi_{\text{rref}} i_{qs\text{ref}}. \tag{37}$$

The reference current i_{qs} is determinated by the following expression:

$$i_{qs\text{ref}} = \left(\dot{\omega}_{\text{rref}} + C_r\frac{p}{j} + \frac{K_f}{j}\omega_r + K_{fs\omega}\text{T2FLC}(S_\omega)\right)\frac{j}{p^2}\frac{L_m + L_r}{L_m\phi_{\text{rref}}}. \tag{38}$$

Step 2: *Current regulators*

In this step, four new errors of the components of the stator current are given by

$$\begin{cases} S_{ds1} = i_{ds1\text{ref}} - i_{ds1}, \\ S_{ds2} = i_{ds2\text{ref}} - i_{ds2}, \\ S_{qs1} = i_{qs1\text{ref}} - i_{qs1}, \\ S_{qs2} = i_{qs2\text{ref}} - i_{qs2}. \end{cases} \tag{39}$$

The augmented Lyapunov function for the second step is given by

$$V_2 = \frac{1}{2}(S_\omega^2 + S_\phi^2 + S_{ds1}^2 + S_{ds2}^2 + S_{qs1}^2 + S_{qs2}^2). \tag{40}$$

We take note that V_2 is chosen in such a way that it permits in achieving the control law.

The derivative of the positive definite function V_2 is

$$\dot{V}_2 = S_\omega \dot{S}_\omega + S_\phi \dot{S}_\phi + S_{ds1}\dot{S}_{ds1} + S_{ds2}\dot{S}_{ds2} + S_{qs1}\dot{S}_{qs1} + S_{qs2}\dot{S}_{qs2}. \tag{41}$$

By applying the Lyapunov stability theorem as in the first step, we obtain

$$\begin{cases} \dot{S}_{ds1} = \dot{i}_{ds1\text{ref}} - \dfrac{1}{L_{s1}}\{V_{ds1} - R_{s1}i_{ds1} + \omega_s(L_{s1}i_{qs1} + T_r\phi_{\text{rref}}\omega_{\text{glref}})\}, \\ \dot{S}_{ds2} = \dot{i}_{ds2\text{ref}} - \dfrac{1}{L_{s2}}\{V_{ds2} - R_{s2}i_{ds2} + \omega_s(L_{s2}i_{qs2} + T_r\phi_{\text{rref}}\omega_{\text{glref}})\}, \\ \dot{S}_{qs1} = \dot{i}_{qs1\text{ref}} - \dfrac{1}{L_{s1}}\{V_{qs1} - R_{s1}i_{qs1} - \omega_s(L_{s1}i_{ds1} + \phi_{\text{rref}})\}, \\ \dot{S}_{qs2} = \dot{i}_{qs2\text{ref}} - \dfrac{1}{L_{s2}}\{V_{qs2} - R_{s2}i_{qs2} - \omega_s(L_{s2}i_{ds2} + \phi_{\text{rref}})\}. \end{cases} \tag{42}$$

Finally, by putting equivalence between system of (42) and system of (24), we obtain (43) which represents the real control

$$\begin{cases} V_{ds1} = L_{s1}(K_{fsds1}\text{T2FLC}(S_{ds1}) + \dot{i}_{ds1\text{ref}}) - R_{s1}i_{ds1} + \omega_s(L_{s1}i_{qs1} + T_r\phi_{\text{rref}}\omega_{\text{glref}}), \\ V_{ds2} = L_{s2}(K_{fsds2}\text{T2FLC}(S_{ds2}) + \dot{i}_{ds2\text{ref}}) - R_{s2}i_{ds2} + \omega_s(L_{s2}i_{qs2} + T_r\phi_{\text{rref}}\omega_{\text{glref}}), \\ V_{qs1} = L_{s1}(K_{fsqs1}\text{T2FLC}(S_{qs1}) + \dot{i}_{qs1\text{ref}}) - R_{s1}i_{qs1} - \omega_s(L_{s1}i_{ds1} + \phi_{\text{rref}}), \\ V_{qs2} = L_{s2}(K_{fsqs2}\text{T2FLC}(S_{qs2}) + \dot{i}_{qs2\text{ref}}) - R_{s2}i_{qs2} - \omega_s(L_{s2}i_{ds2} + \phi_{\text{rref}}). \end{cases} \tag{43}$$

We can write Eq. (43) as follows:

$$\begin{aligned} \dot{V}_2 = {} & S_\omega(-K_\omega\text{T2FLC}(S_\omega)) + S_\phi(-K_\phi\text{T2FLC}(S_\phi)) \\ & + S_{ds1}(-K_{fsds1}\text{T2FLC}(S_{ds1})) + S_{ds2}(-K_{fsds2}\text{T2FLC}(S_{ds2})) \\ & + S_{qs1}(-K_{fsqs1}\text{T2FLC}(S_{qs1})) + S_{qs2}(-K_{fsqs2}\text{T2FLC}(S_{qs2})). \end{aligned} \tag{44}$$

The chosen law for the attractive surface of (41) stratifying the necessary condition of sliding $(S_i \cdot \dot{S}_i) < 0$ obtained in (44) is

$$s_i = -k_{fsi}\text{T2FLC}(s_i). \tag{45}$$

As for the IT2FBSMC approach, we must find a control law to reach it and stay thereafter:

$$u = u_{\text{eq}} + u_s, \tag{46}$$

where u_{eq} is the equivalent control. It makes the derivative of the sliding surface equal to zero to stay on the sliding surface, u_s is the discontinuous control.

The condition to stay on the sliding surface is $\dot{s}_i = 0$; therefore, the equivalent control is

$$\begin{cases} u_{\text{eq}\omega} = \dfrac{j}{p^2}\dfrac{L_m + L_r}{L_m \phi_{\text{rref}}}\left(\dot{\phi}_{\text{rref}} + \dfrac{R_r}{L_m + L_r}\phi_r\right), \\ u_{\text{eq}\phi} = \dfrac{L_m + L_r}{R_r L_m}\left(\dot{\omega}_{\text{rref}} + C_r\dfrac{p}{j} + \dfrac{K_f}{j}\omega_r\right), \\ u_{\text{eq}ds1} = L_{s1}\dot{i}_{ds1\text{ref}} - R_{s1}i_{ds1} + \omega_s(L_{s1}i_{qs1} + T_r\phi_{\text{rref}}\omega_{\text{glref}}), \\ u_{\text{eq}ds2} = L_{s2}\dot{i}_{ds2\text{ref}} - R_{s2}i_{ds2} + \omega_s(L_{s2}i_{qs2} + T_r\phi_{\text{rref}}\omega_{\text{glref}}), \\ u_{\text{eq}qs1} = L_{s1}\dot{i}_{qs1\text{ref}} - R_{s1}i_{qs1} - \omega_s(L_{s1}i_{ds1} + \phi_{\text{rref}}), \\ u_{\text{eq}qs2} = L_{s2}\dot{i}_{qs2\text{ref}} - R_{s2}i_{qs2} - \omega_s(L_{s2}i_{ds2} + \phi_{\text{rref}}). \end{cases} \tag{47}$$

At this present stage, the control discontinuous control law u_{si} is designed as:

$$\begin{cases} u_{s\omega} = \dfrac{j}{p^2}\dfrac{L_m + L_r}{L_m \phi_{\text{rref}}}(K_{fs\omega}\text{T2FLC}(S_\omega)), \\ u_{s\phi} = \dfrac{L_m + L_r}{R_r L_m}(K_{fs\phi}\text{T2FLC}(S_\phi)), \\ u_{sds1} = L_{s1}K_{fsds1}\text{T2FLC}(S_{ds1}), \\ u_{sds2} = L_{s2}K_{fsds2}\text{T2FLC}(S_{ds2}), \\ u_{sqs1} = L_{s1}K_{fsqs1}\text{T2FLC}(S_{qs1}), \\ u_{sqs2} = L_{s1}K_{fsqs2}\text{T2FLC}(S_{qs2}), \end{cases} \tag{48}$$

where K_{fs} are positive constants.

5. Simulation Results

The proposed control strategy (IT2FBSMC) of the speed and flux regulation of 4.5 kW dual stator induction machine designed in this work has been done and validated by Matlab/Simulink software whose parameters are given in Table 3.

Table 3. DSIM motor parameters.

Item	Symbol	Data
DSIM mechanical power	P_w	4.5 kW
Nominal voltage	V_n	220 V
Nominal current	I_n	6.5 A
Nominal speed	ω_n	300 rad/s
Pole pairs number	p	1
Stators resistances	$R_{s1} = R_{s2}$	3.72 Ω
Rotor resistance	R_r	2.12 Ω
Stators self-inductances	$L_{s1} = L_{s2}$	0.22 H
Rotor self-inductance	L_r	0.006 H
Mutual inductance	L_m	0.3672 H
Moment of inertia	J	0.625 kg · m^2
Friction coefficient	K_f	0.001 Nms/rad
Nominal Frequency	f	50 Hz

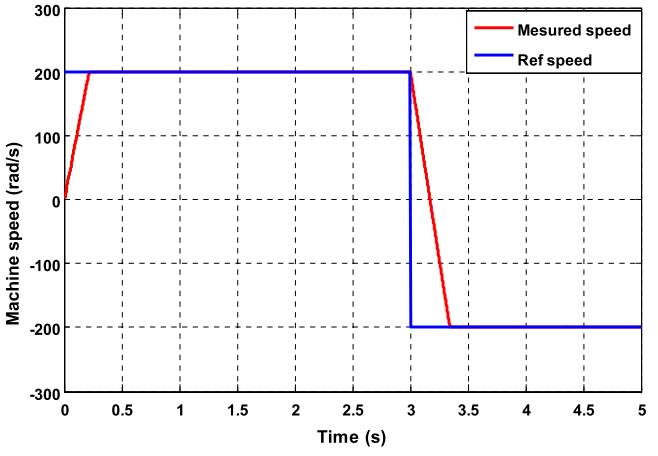

Fig. 5. Simulated results of speed response.

Figures 5–8 show the simulated responses of speed, electromagnetic torque, rotor field and the d–q-axis stator currents, respectively.

The initial rotation speed of the motor is 200 rd/s to 3 s up to −200 rd/s during a period of 0.3 s and after it is fixed to −200 rd/s while the other parameters are held constant. The initial load torque of the motor 14 N · m is abruptly applied at 2 s (Fig. 6), until the end and pursued by an inversion of speed reference in ±200 rd/s at 3 s.

The torque rises quickly when the load disturbance torque increases from 0 to 14 N · m (Fig. 6), this increase shows the effectiveness of the proposed control in terms of load disturbance rejection, on the other hand, the torque decreases quickly

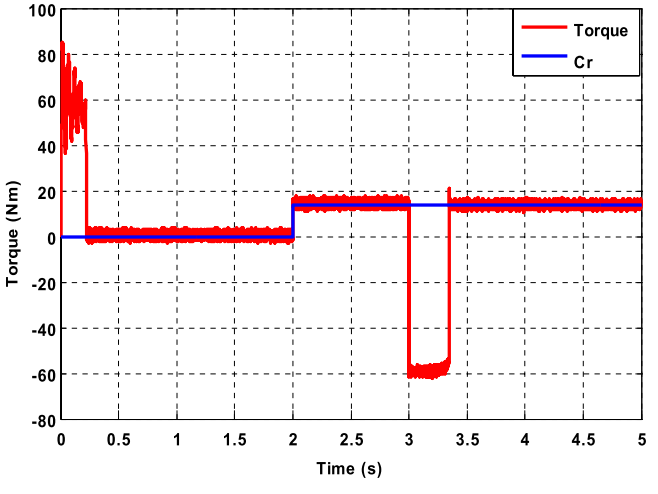

Fig. 6. Simulated results of torque under a load $C_r = 14\,\mathrm{N}\cdot\mathrm{m}$ in 2 s.

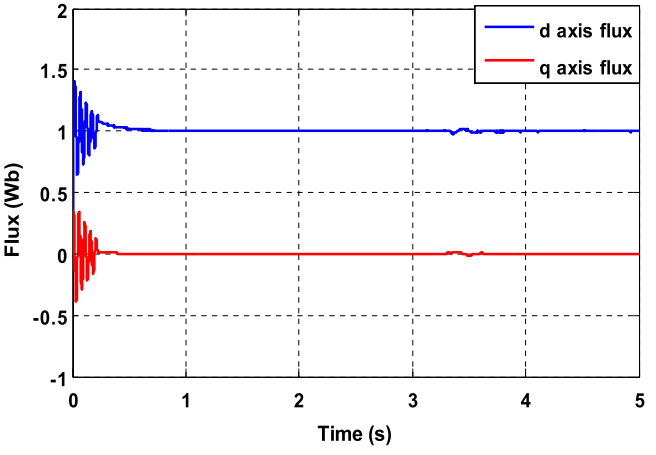

Fig. 7. Simulated results of rotor flux.

to attain the commanded value, once the speed degraded and reaches the value $-200\,\mathrm{rd/s}$, thereafter, the torque settles to provide only the losses of the machine performances.

In Fig. 7, the decoupling of torque–flux is maintained in permanent mode.

Figure 8 shows that the response of the current of the q-axis which controls the torque is similar to electromagnetic torque, whereas the current of the d-axis which controls the flow of the rotor remains constant.

Those results confirm the high performance of the proposed controller and demonstrate the robustness under various operating conditions as well as assure global stability of this machine.

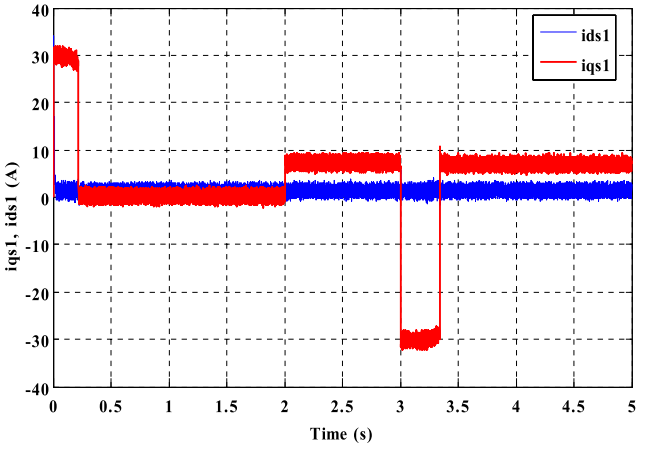

Fig. 8. Simulated results of currents stator (i_{qs1}, i_{ds1}) under a load $Cr = 14\,\mathrm{N}\cdot\mathrm{m}$ in $2\,\mathrm{s}$.

6. Conclusion

In this paper, a control strategy based on interval type-2 fuzzy and backstepping sliding mode (IT2FBSMC) has been proposed for a class of multi-input multi-output nonlinear system (DSIM) in the presence of bounded internal and external disturbances. This combination has been used for deriving the desired thrusts to achieve the required control performance and to eliminate the chattering phenomenon. The effectiveness of the proposed hybrid nonlinear control is validated using Matlab/Simulink. The obtained results show good performances and assure global stability, it allows having fast response without overtaking, settling time in speed response and completing decoupling between the flux and the torque. Moreover, the proposed IT2FBSMC is considered as a major step in the evolution of intelligent control. Finally, the experimental implementation of the proposed control scheme will be addressed in the future work.

References

1. Z. Tir *et al.*, Fuzzy logic field oriented control of double star induction motor drive, *Electr. Eng.* **99** (2017) 495–503.
2. Z. Tir, O. P. Malik and A. M. Eltamaly, Fuzzy logic based speed control of indirect field oriented controlled double star induction motors connected in parallel to a single six-phase inverter supply, *Electr. Power Syst. Res.* **134** (2016) 126–133.
3. B. Meliani and A. Meroufel, A neural network based speed control of a dual star induction motor, *Int. J. Electr. Comput. Eng.* **4** (2014) 952–961.
4. D. Hadiouche, H. Razik and A. Rezzoug, Study and simulation of space vector PWM control of double-star induction motors, in *Proc. VII IEEE Int. Power Electronics Congress*, Vol. 7, 2000, Acapulco, Mexico, pp. 42–47.
5. B. Meliani, A. Meroufel and H. Khouidmi, Fuzzy gain scheduling of PI controller for dual star induction machine fed by a matrix converter, *Carpathian J. Electron. Comput. Eng.* **5** (2012) 77–82.
6. S. Lekhchine, T. Bahi and Y. Soufi, Indirect rotor field oriented control based on fuzzy logic controlled double star induction machine, *Int. J. Electr. Power Energy Syst.* **57** (2014) 206–211.
7. B. Ghalem and A. Bendiabdallah, Six-phase matrix converter fed double star induction motor, *Acta Polytech. Hung.* **7** (2010) 163–176.
8. L. Benalia, Control of a double feed and double star induction machine using direct torque control, in *Torque Control*, ed. M. T. Lamchich, Chap. 5 (In Tech, Croatia, 2011), pp. 113–126.
9. B. Ghalem and A. Bendiabdallah, A comparative study between two control strategies for matrix converte, *Adv. Electr. Comput. Eng. J* **9** (2009) 23–27.
10. A. Gholami and A. H. D. Markazi, Direct adaptive fuzzy sliding observation and control, *Trans. Canad. Soc. Mech. Eng.* **36** (2012) 329–342.
11. H. Kouki, M. Ben Fredj and H. Rehaoulia, SVPWM control strategy to minimize circulation harmonic currents for VSI fed double star induction machine, in *Proc. Int. Multi-Conf. IEEE Systems, Signals & Devices (SSD)*, Vol. 12 (IEEE, New York, 2015), pp.1–7.
12. C. Navaneethakkannan and M. Sudha, Comparison of conventional & PID tuning of sliding mode fuzzy controller for BLDC motor drives, in *Proc. Int. Conf. Computer Communication and Informatics (ICCCI 2013)*, Coimbatore (2013), pp. 4–6.

13. S. Zeghlache, D. Saigaa, K. Kara, A. Harrag and A. Bouguerra, Backstepping sliding mode controller improved with fuzzy logic: Application to the quadrotor helicopter, *Arch. Control Sci.* **22** (2012) 255–282.
14. T. Laamayad, F. Naceri, R. Abdessemed and S. Belkacem, A new PI-fuzzy sliding mode controller. Application to the Dual Star Induction Machine (DSIM), in *Proc. Int. Conf. Electronics & Oil*, Ouargla, Algeria, Vol. 1 (2011), pp. 261–266.
15. F. Naceri, T. Laamayad and S. Belkacem, Fuzzy sliding mode speed controller design of induction motor drives, in *Proc. Int. Conf. Industrial Engineering and Operations Management*, Istanbul, Turkey (2012), pp. 1330–1339.
16. H. Amimeur, D. Aouzellag, R. Abdessemedn and K. Ghedamsi, Sliding mode control of a dual-stator induction generator for wind energy conversion systems, *Int. J. Electr. Power Energy Syst.* **42** (2012) 60–70.
17. M. Moutchou, A. Abbou and H. Mahmoudi, Sensorless speed backstepping control of induction machine, based on speed MRAS observer, in *Int. Conf. IEEE Proc. Multimedia Computing and Systems (ICMCS)*, Tangier, Morocco (2012), pp. 1019–1024.
18. M. Moutchou, A. Abbou and H. Mahmoudi, MRAS-based sensorless speed backstepping control for induction machine, using aux sliding mode observer, *Turk. J. Electr. Eng. Comput. Sci.* **23** (2015) 187–200.
19. T. Laamayad, F. Naceri, R. Abdessemed and S. Belkacem, A fuzzy sliding mode strategy for control of the dual star induction machine, *J. Electr. Eng.* **13** (2013) 1–8.
20. M. R. Douiri, O. Belghazi and M. Cherkaoui, Neuro-fuzzy-based auto-tuning proportional integral controller for induction motor drive, *Int. J. Comput. Intell. Appl.* **14** (2015) 1–22.
21. H. Rahali, S. Zeghlache and L. Benalia, Adaptive field-oriented control using supervisory type-2 fuzzy control for dual star induction machine, *Int. J. Intell. Eng. Syst.* **10** (2017) 28–40.
22. T. S. Radwan, Perfect speed tracking of direct torque controlled induction motor drive using fuzzy logic, in *Proc. Int. Conf. Power Electronics and Drives Systems, PEDS, IEEE*, Kuala Lumpur, Malaysia (IEEE, New York, 2005), pp. 38–43.
23. K. Loukal and L. Benalia, Interval type-2 fuzzy gain-adaptive controller of a doubly fed induction machine (DFIM), *J. Fundam. Appl. Sci.* **8** (2016) 470–493.
24. K. Chafaa *et al.*, Direct adaptive type-2 fuzzy control for nonlinear systems, *Int. J. Comput. Intell. Appl.* **6** (2006) 389–411.
25. Q. Liang and J. Mendel, Interval type-2 fuzzy logic systems: Theory and design, *IEEE Trans. Fuzzy Syst.* **8** (2000) 535–550.
26. J. Mendel, *Uncertain Rule-based Fuzzy Logic Systems: Introduction and New Directions*, Vol. 1 (Prentice-Hall, New Jersey, 2001), pp. 1–674.
27. W. Gao and J. C. Hung, Variable structure control of nonlinear systems: A new approach, *IEEE Trans. Ind. Electron.* **40** (1993) 45–50.
28. S. Zeghlache, K. Kara and D. Saigaa, Fault tolerant control based on interval type-2 fuzzy sliding mode controller for coaxial trirotor aircraft, *ISA Trans.* **59** (2015) 215–231.
29. M. Chen and M. Huzmezan, A combined MBPC/2 DOF H^{∞} Controllers for a quadrotor UAV, in *Proc. of the AIAA Guidance, Navigation, and Control Conf. and Exhibit*, Texas, USA (2003), p. 11–14.
30. A. Benallegue, V. Mister and K. M. Sirdi, Exact linearization and non-interacting control of a 4 rotors helicopter via dynamic feedback, in *Proc. Int. Workshop on Robot and Human Interactive Communication*, Bordeaux, France (2001), pp. 586–591.
31. A. Hocine and A. Benalia, Sensorless fault tolerant control for induction motors using: Backstepping strategy and sliding mode observer, in *Proc. Int. Conf. Modeling,*

Identification and Control (ICMIC), Algiers, Algeria, Vol. 8 (IEEE, New York, 2016), pp. 1020–1028.
32. N. Djeghali *et al.*, Sensorless fault tolerant control for induction motors, *Int. J. Control, Autom. Syst.* **11** (2013) 563–576.
33. H. Echeikh *et al.*, Online adaptation of rotor resistance based on sliding mode observer with backstepping control of a five-phase induction motor drives, *Int. J. Power Electron. Drive Syst.* **7** (2016) 648–655.
34. H. Echeikh *et al.*, Non-linear backstepping control of five-phase IM drive at low speed conditions — experimental implementation, *ISA Trans.* **65** (2016) 244–253.